

Producing carbon nanotubes from thermochemical conversion of waste plastics using Ni/ceramic based catalyst

Xiaotong Liu^a, Boxiong Shen^{b*}, Zhentao Wu^{c*}, Christopher M. A. Parlett^{d*}, Zhenan Han^e, Adwek George^b, Peng Yuan^b, Dipesh Patel^a, Chunfei Wu^{a,b*}

^a School of Engineering and Computer Science, Faculty of Science and Engineering, University of Hull, Hull, HU6 7RX

^b School of Energy and Environmental Engineering, Hebei University of Technology, Tianjin, China

^c Aston Institute of Materials Research, School of Engineering and Applied Science, Aston University, Birmingham B4 7ET, UK

^d European Bioenergy Research Institute, Aston University, Birmingham, B4 7ET, UK

^e Wuhan Optics Valley Environmental Technology Co., Ltd, Wuhan City, China 430074

Corresponding authors: Tel: +44 (0) 1482466464, Email: c.wu@hull.ac.uk; Tel: +86 (0) 2260435784, E-mail: shenbx@hebut.edu.cn; Tel: +44 (0) 121204 3353, Email: z.wu7@aston.ac.uk; Tel: +44 (0)1212 044100 c.parlett@aston.ac.uk)

Abstract

As the amount of waste plastic increases, thermo-chemical conversion of plastics provides an economic flexible and environmental friendly method to manage recycled plastics, and generate valuable materials, such as carbon nanotubes (CNTs). The choice of catalysts and reaction parameters are critical to improving the quantity and quality of CNTs production. In this study, a ceramic membrane catalyst (Ni/Al₂O₃) was studied to control the CNTs growth, with reaction parameters, including catalytic temperature and Ni content investigated. A fixed two-stage reactor was used for thermal pyrolysis of plastic waste, with the resulting CNTs characterized by various techniques including scanning electronic microscopy (SEM), transmitted electronic microscopy (TEM), temperature programm oxidation (TPO), and X-ray diffraction (XRD). It is observed that different loadings of Ni resulted in the formation of metal particles with various sizes, which in turn governs CNTs production with varying degrees of quantity and quality, with an optimal catalytic temperature at 700 °C.

Keywords: Plastics waste; Carbon nanotubes; ceramic membrane; Nickel; catalyst

31 **1. Introduction**

32 There was more than 4.3 million tonnes plastics waste generated in the UK in 2015 [1],
33 the disposal of waste plastic causes environmental concerns. Therefore, careful
34 management is needed to minimize the environmental impact of plastic waste. As waste
35 plastic contains a high value of energy, recycle and recovery methods are encouraged
36 compared to landfilling. Thermochemical recycling of waste plastics which converts
37 plastics materials into other valuable materials, refers to an advanced technology
38 process [2]. During this process, hydrogen-rich syngas is generated at high pyrolysis
39 temperature ($>800\text{ }^{\circ}\text{C}$) or gasification of waste plastics. For example, Erkiaga et al. [3]
40 generated a syngas stream rich in H_2 from pyrolysis of plastic waste (high density
41 polyethylene) with Ni catalysts. Syngas has wide applications, including directly
42 combusted for the production of heat and power, or conversion into liquid fuels through
43 Fishcher-Tropsch process [4]. Recently, co-production of carbon nanotubes (CNTs)
44 from pyrolysis or gasification of waste plastics has also attracted interest. CNTs were
45 first introduced in 1952, and further inspired by Iijima [5, 6]. CNTs have extraordinary
46 properties, including high mechanical strength, good electrical and thermal
47 conductivity, and there promising potential applications. However, the high price
48 ($\sim\$85\text{-}95/\text{kg}$) has significantly prohibited the applications of CNTs [7]. Converting
49 plastic waste to CNTs provides a promising alternative and economic flexible method
50 to generate such high valuable material.

51 Chemical vapour deposition (CVD) is the current method of choice and widely utilised

52 to produce CNTs from plastics, due to its simplicity and low cost. This method used
53 hydrocarbon gases as carbon sources and catalysts particles to nucleate the CNTs
54 growth [8]. For example, Park et al. [9] optimized operation conditions with Ru-based
55 catalysts from waste plastic, in order to decrease the coke formation and increase the
56 carbon conversion. Liu et al. [10] used a two-stage reactor to convert PP into CNTs and
57 hydrogen-rich gas with HZSM-5 as catalysts, and an optimum temperature (700°C)
58 was proposed. Wu et al. studied the production of CNTs and syngas study from different
59 types of plastics with varies of catalysts [11-14].

60 It is known that catalysts play a key role in the growth of CNTs. The catalysts used for
61 CVD synthesis of CNTs formation normally consist of a transition metal and support.
62 The transition metal nanoparticles are employed either in oxide or metallic forms.
63 Nickel, iron, and cobalt are reported as the most effective catalysts due to the high
64 solubility and high diffusion rate of carbon. For example, Lee et al [15] compared the
65 performance of Ni, Co and Fe based catalysts for CNTs growth from mixed gases. Fe
66 was found to be the most active catalyst for CNTs growth under CO/NH₃ gas flow with
67 a ratio of 18. Apart from these common catalysts, there are also some other types of
68 metals that have been studied for CNTs formation, such as Cu, Ru, Mn and Cr. Catalysts
69 for CNTs formation also need an appropriate material as support [16]. Various
70 substrates have been used for CVD of CNTs synthesis, such as silicon dioxide [14],
71 alumina [17], quartz, calcium carbonate [18], and zeolite [19]. Fe-Co bimetallic
72 catalysts supported on CaCO₃ were used as catalysts by Mhlanga et al. [18] to improve
73 the quality of CNTs with decreasing synthesis time from acetylene. CNTs with outer

74 diameter of 20-30 nm and inner diameter about 10 nm have been successfully produced.

75 Furthermore, many researchers are working on catalyst development to improve the

76 quality of CNTs [13, 20-24].

77 Recently, membrane supported catalysts have emerged, and can be used as a template

78 for CNTs growth to control parameters such as diameter, length, and wall thickness

79 [25]. For example, Golshadi et al. [25] investigated the influence of process parameters

80 (temperature and flow rate) on the CNTs formation (tube wall thickness, CNTs

81 morphology and carbon deposition rate) using anodic aluminum oxidize (AAO)

82 template. It was reported that the yield and wall thickness of the produced CNTs were

83 increased with the increase of reaction temperature to 750 °C; however, further

84 increasing the temperature resulted in a lower production of CNTs. In addition an

85 optimum of gas flow rate was reported for the production of CNTs. Well-aligned CNTs

86 have also been synthesized on glass template from acetylene gas by plasma-enhanced

87 CVD process [26]. Zeolites have also been employed as controlling agents during CNTs

88 growth [27].

89 According to our previous study, AAO membrane catalysts could be used for

90 controlling and improving the quality of CNTs formation [28]. Ceramic membrane

91 (alumina based) was selected as template in this study. This ceramic membrane was

92 provided by AIMR, Aston University, and the properties were studied in Lee's paper

93 [29]. In Lee's paper, ceramic membrane was reported having micro-channel structure,

94 which was similar to our previous research on AAO membrane [28] [29]. This micro-

95 channel structure could control the metal particle loaded inside the membrane and
96 consequently control the CNTs diameter. However, the yield of CNTs production using
97 AAO based membrane is low as AAO is difficult to be manufactured in a large scale.
98 Ceramic membrane has been commercially produced and also has other good properties,
99 such as high temperature stability, mechanical strength, chemical stability, and low cost
100 [30, 31]. These properties make ceramic materials one of the best catalytic supports in
101 the fields of environmental and energy research [31]. Quan et al. produced high quality
102 syngas from biomass fuel gas over NiO/porous ceramic catalysts [32]. And Gao et al.
103 studied steam reforming of biomass tar for hydrogen production using NiO/ceramic
104 foam as catalysts [33]. Membrane catalysts have also shown superior catalytic stability
105 over equivalent powder [34].

106 The quality of CNTs can significantly affect and limit their applications. For example,
107 An et al. [35] synthesized CNT composite from the catalytic decomposition of
108 acetylene over Fe/aluminum ceramic catalyst. It was reported that the CNT content
109 increased with the increase of Fe content. The mechanical properties of the produced
110 composite material was also enhanced with the increase of CNTs formation. Flahaut et
111 al. [36] prepared Fe-Al₂O₃ ceramics with and without CNTs to study composites
112 properties, and they found those contained higher quantities of CNTs and much less
113 nanofibers were good electric conductors. Therefore, experimental conditions (both
114 reaction temperature and Ni loading) were studied to determine the optimal conditions
115 for the production of high quality CNTs, which is reflected by a narrow distribution of
116 CNTs diameter.

117

118 **2. Experimental**

119 2.1 Materials preparation

120 High density polyethylene plastics (HDPE) pellets with high purity (~ 90%) and a
121 diameter around 2 mm were provided by Poli Plastic Pellets Ltd. Ceramic membrane
122 used in this study was made of aluminium oxide, and with 1mm thickness and 30mm
123 diameter provided by AIMR, Aston University. The original ceramic membrane
124 preparation and formation method was described in Lee's paper [29]. It is noted that
125 the BET surface area of the membrane is below 10 m²/g. Impurities such as
126 polyethersulfone was used as binder for membrane preparation. The required amounts
127 (0.025g for 0.1/ceramic, 0.125g for 0.5/ceramic, 0.251g for 1.0/ceramic, 0.508g for 2.0
128 ceramic) of Ni (NO₃)₂.6H₂O were dissolved in 5ml ethanol, the mixture liquid was
129 loaded on each membrane (~1.32g) by dropping the precursors into the membrane. The
130 obtained wet Ni/ceramic membrane was dried in the oven at 100°C for 24h, then
131 calcined in air at 800 °C with 10 °C min⁻¹ heating rate for 3 hours. It is noted that the
132 Ni/ceramic catalysts prepared from using 0.1, 0.5, 1.0 and 2.0 mol L⁻¹ Ni (NO₃)₂.6H₂O
133 was assigned as 0.1/ceramic, 0.5/ceramic, 1.0/ceramic and 2.0/ceramic, respectively in
134 this paper.

135 2.2 CNTs synthesis from catalytic pyrolysis of plastics

136 A two-stage catalytic thermal-chemical conversion reaction system (Fig. 1) consisting
137 of a plastic pyrolysis stage and a catalytic gasification stage. In each experiment, about

138 1 g HDPE was pyrolysed at around 500 °C at the first stage, Different reaction
139 temperatures were used in the second stage (600 °C, 700 °C, and 800 °C). N₂ was used
140 as carrier gas with 100 ml min⁻¹ flow rate. The total reaction time was 60 mins. The
141 system was then slowly cooled down to the room temperature with continuous 100 ml
142 min⁻¹ N₂ gas. The reacted Ni/ceramic membrane catalyst including the grown CNTs
143 were collected for further characterizations. The effect of pyrolysis temperature and the
144 content of Ni on ceramic membrane were studied in relative to their influences on the
145 growth of CNTs.

146 2.3 Sample characterization

147 A scanning electron microscope (SEM) Stereoscan 360 and a high resolution
148 transmission electron microscope (TEM) JEOL 2010 were used to analyse the surface
149 and the cross-section morphology of the fresh Ni/ceramic membrane. According to
150 TEM results, the distribution of diameters of catalyst particles were further analyzed by
151 Image J software. Sample crystallinity was evaluated by powder X-ray diffraction
152 (XRD), using Stoe IPDS2 software, with elemental analysis assessed by inductively
153 coupled plasma mass spectrometry (ICP-MS), ThermoScientific iCAP 7000 ICP
154 spectrometer after complete sample digestion in conc. Nitric acid. In addition,
155 temperature program reduction (TPR) was carried out on a Quantachrome Chem BET
156 3000 system, with samples heated from 50 °C to 700 °C at 10 °C min⁻¹ under flowing
157 H₂ (10 ml min⁻¹), to observe the catalytic metal reduction.

158 CNTs formation on the Ni/ceramic after reaction was also investigated by SEM and

159 TEM. Distribution of CNTs diameters according to TEM results was carried out using
160 Image-J software. Temperature programmed oxidation (TPO) of the reacted Ni/ceramic
161 was analysed to obtain the information of carbon formation on the reacted catalyst.

162

163 **3. Results and discussion**

164 3.1 Characterization of fresh Ni/ceramic catalyst

165 Fresh catalysts before reaction with different Ni loadings have been analysed by SEM,
166 TEM, ICP, XRD and TPR, respectively. SEM results of the surface and the cross section
167 of the fresh Ni/ceramic catalyst are shown in Fig. 2A and 2B, respectively. The surface
168 and cross-section show a similar structure; porous structure can be clearly observed
169 from both pictures. Therefore, SEM images on the surface of materials are used for
170 following discussion. Based on the XRD results (Fig. 3), the original ceramic
171 membrane without Ni loading shows diffraction peaks of Al_2O_3 [37], indicating the
172 nature of the ceramic is Al_2O_3 . NiO peaks appear at 63° and 76° , respectively, for the
173 catalyst with different Ni contents loadings [14]. Two NiAl_2O_4 peaks appear at around
174 37° and 77° [38]. ICP results as shown in Table 1 further indicate that the content of
175 Ni element increased from 0.25 to 3.3 wt. % with the increase of Ni loading. Fig. 4
176 shows the TEM results (A-D) for the Ni/ceramic samples. The distribution of NiO
177 diameters was also calculated according to TEM results for the catalyst with different
178 Ni loadings. Small amount of NiO particles was observed on the surface of the
179 0.1/ceramic, which has particles with 11.4 ± 2.4 nm diameter, with NiO diameter

180 correlating with metal loading, in agreement with the literature[11], resulting in average
181 particle size of 35.2 ± 3.5 nm for the 2.0/ceramic (Fig.3 D).

182 TPR results of the fresh Ni/ceramic catalysts are shown in Fig. 5. A major reduction
183 temperature for all the catalysts occurred between 370 and 450°C, assigned to the
184 reduction of NiO particles [11]. As shown in Fig. 5, the catalysts were further reduced
185 at 550 °C which is suggested to the reduction of Ni spinel as observed from the XRD
186 analysis (Fig.3).

187 3.2 Carbon nanotubes production

188 Two reaction parameters using ceramic membrane catalysts with different Ni contents
189 loading were investigated in relation to the effect on the CNTs formation from plastics
190 waste. Table 2 is a summary of different reaction parameters (Ni content and reaction
191 temperature) and CNTs formation analysis (amount of amorphous carbon, filamentous
192 carbon and CNT average diameter). When the effect of reaction temperature (600, 700,
193 and 800 °C) was studied, the 0.5/ceramic catalyst was used. When the effect of Ni
194 content (0.1, 0.5, 1.0 and 2.0) was studied, thermochemical conversion of waste HDPE
195 was investigated at 700 °C.

196 CNTs formation from thermochemical conversion of plastics waste in this study was
197 investigated according to both quantitative analysis and qualitative analysis. The
198 quantitative analysis of CNTs was further discussed based on the yields of amorphous
199 carbons and filamentous carbons which was obtained by TGA-TPO analysis of the
200 spent catalysts (Fig. S1 and S2). It is assumed that the oxidation temperature below

201 550 °C was assigned to amorphous carbons and the oxidation above 550 °C in TPO
202 was assigned to filamentous carbon (assumed as CNTs in this work) [39], two different
203 types of carbon has been separated and analysed by vertical black imaginary line (Fig.
204 S1 and S2). The total carbon yield could be represented by X axis 'the weight loss' of
205 catalyst in relation to the initial catalyst weight. The fractions of the two different types
206 of carbons in relation to the weight of reacted catalysts are summarized in Table 2.

207 In addition, the quality of CNTs production is analysed and discussed mainly based on
208 the distribution of CNTs diameters and their standard deviations. The average diameter
209 of CNTs is calculated according to SEM and TEM results using Image J, and
210 summarized in Table 2 (shown in Fig. S3). The standard deviation (SD) number is used
211 as a main factor to identify the quality of CNTs formation in this study. In addition, the
212 ratio of filamentous and amorphous carbon was also discussed in following sections to
213 obtain the optimum reaction parameter for CNTs formation. A better quality of CNTs
214 is identified with a smaller SD number and higher ratio of filamentous and amorphous
215 carbon in this paper.

216 3.3 Effect of reaction temperature on CNTs growth

217 The effect of reaction temperature on the growth of CNTs through thermal conversion
218 from HDPE using Ni/ceramic catalysts is discussed in this section. Three different
219 reaction temperatures (600°C, 700°C and 800°C) were investigated using the 0.5/
220 ceramic catalyst. Scanning electron microscope (SEM), transmitted electron
221 microscope (TEM), temperature program oxidation (TGA-TPO and DTG-TPO)

222 analysis were carried out to the reacted CNTs/catalysts. For SEM results (Fig.6 A-C),
223 a small amount of uninform, short filamentous carbons were observed at 600°C
224 (Fig.6A). CNTs with a diameter around 10 nm and a length around 10 μm is observed
225 at catalytic reaction temperature of 600 °C. This results is similar to literature where
226 Ni/Al₂O₃ was used for producing CNTs from waste plastics [14].

227 With the increase of reaction temperature to 700°C (Fig.6B), a large amount of
228 filamentous carbons with long length are found on the ceramic membrane. However,
229 when the reaction temperature was further increased to 800°C, only a few filamentous
230 carbons could be observed on the surface of the catalyst (Fig.6C). The SEM results of
231 the reacted catalyst were further supported by TEM analysis (Fig. 6 i-iii). CNTs with
232 diameter 21.2 ± 5.6 and 16.9 ± 4.3 nm were clearly observed in Fig. 6 i and ii,
233 respectively. It is difficult to find CNTs on the catalyst reacted at 800 °C (Fig.6 iii).
234 Therefore, it is suggested that 700 °C is an optimal reaction temperature for the
235 formation of CNTs from waste plastics in this work. Similar results were reported by
236 Li et al [40], who studied various temperatures from 600°C to 1050°C for CNTs
237 production from C₂H₂ with Fe/SiO₂ catalysts. They reported minimal CNTs yield at
238 either low (600°C) or high (1050°C) temperature.

239 This result is further supported by carbon production analysis (Table 2). For amorphous
240 carbons (oxidation temperature below 550 °C), the yield was decreased from 2.1 to 1.2
241 wt. %, when the temperature increased from 600 °C to 700 °C. This result is consistent
242 with the SEM analysis (Fig. 6), where amorphous carbons could be clearly observed on

243 the reacted catalyst tested at 600 °C. Furthermore, the formation of CNTs was reduced
244 from 7.2 wt. % and 1.2 wt. % when the reaction temperature was increased 600°C and
245 800°C. DTG-TPO results (Fig.7) with DCS (Differential Scanning Calorimetry)
246 showed that the oxidation peak moved to higher temperature with the increase of
247 experimental temperature from 600°C and 700°C, indicating that the CNTs might be
248 more crystalized at 700°C reaction temperature. Similar results were also reported by
249 Hornyak et al. [41], who investigated the template synthesis of CNTs formation on
250 porous alumina membrane (PAM) from propylene gas with Co-based catalysts. They
251 reported that amorphous carbon was formed at around 550°C, while CNTs was formed
252 at temperature higher than 800°C. The starting temperature for CVD synthesis of CNTs
253 was normally over 500°C [42-44].

254 It is suggested that the effect of reaction temperature on CNTs synthesis by CVD was
255 mainly related to carbon source and catalytic sites. CNTs growth can be described as
256 following steps, first carbon atoms from the dissociation of hydrocarbons dissolve into
257 the catalytic metal sites. The diffused carbon atoms form graphitic sheets on the surface
258 of metal particles [45]. The diffusion of carbon atoms is a main factor to determine the
259 CNTs formation. The increasing temperature can promote the diffusion rate of carbon
260 atoms, as a result, CNTs are synthesised with less defect. Lee et al. [46] and Mishra et
261 al. [47] also reported that an increase of temperature promoted the diffusion and
262 reaction rates of carbons, resulting in the enhanced formation of CNTs. In addition, Wu
263 and Williams [48] reported that at high temperature, more reactive carbon sources were
264 produced from pyrolysis of waste plastics. Therefore, in this study, less amorphous

265 carbons were form at 700°C compared to 600°C, which supported by SEM and TPO
266 analysis. Similar results were reported by Acomb et al. [49] who carried out the effect
267 of growth temperature (700 °C, 800 °C, and 900 °C) on the CNTs production using low
268 density polyethylene (LDPE) with Fe/Al₂O₃ as catalyst. They found that a lower
269 temperature produced less fraction of CNTs.

270 However, when the reaction temperature is too high, the sintering of catalytic sites
271 could occur, which is responsible for the deactivation of catalysts [43]. Also, the excess
272 of carbon atoms accumulated on the surface of catalyst could encapsulate catalytic sites
273 causing catalyst deactivation. For example, Hanaei et al. [50] investigated the influence
274 of reaction temperatures (550°C-950°C) on CNTs from acetone with Fe-Mo/Al₂O₃
275 catalysts. 750°C was reported as an ideal temperature as the deactivation of catalysts
276 occurred at higher temperature. Toussi et al. [51] reported the similar conclusion on
277 CNTs synthesis form ethanol deposited on Fe-Mo-MgO catalyst; when temperature was
278 lower than 750°C, few CNTs could be produced. And the optimum growth of CNTs
279 was reported at 850°C. Kukoitsky et al. [52] reported an optimal temperature of 700°C
280 for the growth of CNTs from polyethylene with Ni-based catalyst at 700°C; as narrow
281 size distribution of CNTs was found at 700°C than those grown at 800°C, due to the
282 loss of catalytic activity for CNTs forming at high temperature. In this study, it is
283 noticed that there was little CNTs formed at 800°C (Fig. 6 and 7), which we attribute to
284 loss of catalytic active sites at high temperature due to sintering As shown in Fig. 6iii,
285 almost no CNTs production could be observed from TEM results. The diameter of NiO
286 particles before reaction was 17.9±4.4 nm (Fig. 4B), however, large amount of large

287 catalytic particles with diameter 52-78 nm could be observed after reaction (Fig. 6iii).
288 Overall, Fig. 8 summarizes the trends of SD of CNTs diameter and ratio of filamentous
289 amorphous carbon as increasing reaction temperature. CNTs show the smallest SD and
290 highest filamentous / amorphous carbon ratio at 700 °C reaction temperature. Therefore,
291 700°C was assumed as the optimum temperature for this study.

292 3.4 Effect of Ni content on the production of CNTs

293 In this section, thermochemical conversion of waste HDPE was investigated in the
294 presence of Ni/ceramic catalysts with different Ni contents at 700°C. Fig.8 showed the
295 SEM results and corresponding TEM results for the filamentous carbon production
296 using the Ni/ceramic catalysts. With the increase of Ni loading, more filamentous
297 carbons could be observed from SEM results. In particular, for the reacted 0.1/ceramic
298 catalyst, the formation of filamentous carbons can be barely found. It is indicated that
299 the 0.1/ceramic and 0.5/ceramic catalysts might have small amount of active metals
300 loaded on the ceramic membrane. TEM results (Fig.8 i-v) further proved that the
301 filaments carbons are mostly CNTs. The average diameter of CNTs (Table 2) was
302 analysed according to the TEM results. It could be noticed that the diameter of CNTs
303 increased with an increase of Ni content. The 0.1/ceramic had the smallest diameter
304 15.7 ± 3.6 nm, and the 2.0/ceramic had the largest diameter 24.9 ± 2.3 nm, in close
305 agreement with the average sizes of the NiO nanoparticles. The changes of diameters
306 of CNTs showed a similar trend with the metal particles size as shown in Fig. 10, where
307 the particle size of NiO was increased with the increase of metal loading. Similar results

308 were also found by other researchers [53]. Sinnott et al. [53] studied the effect of Fe
309 content on the diameter of CNTs produced from ferrocene-xylene mixture through
310 chemical vapour deposition. They reported that the average Fe particle size was
311 decreased from 35.3 to 28.2 nm with a decrease of Fe content from 0.75 to 0.075 at%
312 and the lower Fe content resulted in the production of less CNTs. Li et al. [54]
313 synthesised CNTs from methane and hydrogen mixture using Fe₂O₃-based catalysts
314 with a range of 1-2nm and 3-5 nm respectively. CNTs with diameters of 1.5±0.4 nm
315 and 3.0±0.9 nm were produced, respectively. The CNTs could be diffused by catalytic
316 metal particles during growth process, therefore, the size of metal particles determine
317 the diameter of filamentous carbons [53]. For example, Cheung et al. [55] used iron
318 nanoparticles with average diameters of 3, 9, and 13nm to grow CNTs with average
319 diameters of 3, 7, and 12 nm from ethylene, respectively.

320 The size of metal particles have also been reported to affect the activity of catalysts and
321 the formation of CNTs [55-60]. In addition, loading various amounts of metal on
322 catalyst normally results in the formation of catalyst with various metal particle sizes,
323 as obtain in this work, to control the production of CNTs. Daudouin et al. increased the
324 Ni loading from 1.0 wt.% to 18.5 wt.% to increase the catalytic particle sizes from 1.6
325 to 7.3 nm [61]. The diameter of metal particles was increased with the increase of metal
326 loading. In addition, CNTs with larger diameters were produced with the increase of
327 metal loading. However, a maximum diameter of CNTs should be expected, when the
328 loading of metal in the catalyst is too high. For example, Chen et al. [62] referred to an
329 optimally size of catalyst which could produce an optimum growth rate and a high yield

330 of carbon nanofibers (CNFs). They reported that smaller ($< 20\text{nm}$) Ni crystals caused a
331 slow growth of CNFs and a fast deactivation of catalyst. However, when the metal
332 particles were larger than 60nm , the rate of CNFs growth was prohibited due to the low
333 surface area of active sites. Danafar et al.[57] studied Fe-Co/Al catalysts with 6 ranges
334 of metal particle sizes to study the influence on the synthesis of CNTs from ethanol.
335 They found that the catalyst with $10\text{-}20\ \mu\text{m}$ metal particles produced about 30% higher
336 carbon yield than the catalyst having the largest catalytic particles. It is reported that
337 the catalysts with smaller diameters had larger breaking through capacities during
338 frontal diffusion (shorter diffusion path length). In addition, the catalyst with large
339 metal particle size produced more amorphous carbons and uninform CNTs, as the
340 stability of metal agglomerates decreased with increasing particle sizes.

341 According to Table 2 and DTG-TPO (Fig. 11) analysis of the reacted catalysts with
342 different Ni loadings, a maximum production of CNTs was obtained in the presence of
343 the 1.0/ceramic catalyst. CNTs production was increased from 3.1 to 9.4 wt %, when
344 the catalyst was changed from the 0.1/ceramic to the 1.0/ceramic. Similar results have
345 been discussed by other researchers. For example, Venegoni et al. [63] studied the effect
346 of Fe content (0.5%, 1%, 2% and 5%) on CNTs growth in the presence of Fe/SiO₂
347 catalysts from a mixture of H₂ and C₂H₄. Catalyst with the most amount of Fe metal
348 content (5% Fe-SiO₂) was least active in relation to the production of CNTs, due to the
349 presence of large metal particles. In addition, it was reported that the active catalytic
350 sites was increased to promote catalytic reactions with increasing catalytic metal
351 content until an optimal value was reached [64]. In this study, the

352 filamentous/amorphous carbon ratio was the highest about 5 with the 0.5/ceramic
353 catalyst used (Fig. 12), then slightly decreased to about 4.7 when the catalyst was
354 changed to the 1.0/ceramic. However, the 0.5/ceramic catalyst showed the highest SD
355 number (Fig. 12). Overall, considering the filamentous/amorphous carbon ratio and SD
356 of CNTs diameter, the 1.0/ceramic catalyst was suggested to be a better candidate for
357 CNTs formation from thermochemical conversion from plastic waste.

358

359 **4. Conclusions**

360 Carbon nanotubes formation from catalytic thermo-chemical conversion of waste
361 plastics using ceramic membrane based catalyst was optimized in this work in relation
362 to metal loading and reaction temperature. An optimum temperature 700° was
363 suggested for Ni-based ceramics membrane. An increase of Ni content on ceramic
364 membrane resulted in increasing diameters of metal particle sizes which could affect
365 the activity of catalysts and the formation of CNTs. The 1.0/ceramic was the optimum
366 candidate for CNTs formation in this study giving the highest fraction of filamentous
367 carbons with the narrowest distribution of CNTs diameter.

368

369 **Acknowledgement**

370 The authors would like to thank The University of Hull, UK and Hebei University of
371 Technology, China for the financial support towards this research work.

372

373 **References**

- 374 [1] WRAP. Plastics Market Situation Report. (Spring 2016).
- 375 [2] S.M. Al-Salem, P. Lettieri, J. Baeyens. Recycling and recovery routes of plastic
376 solid waste (PSW): A review. *Waste Management*. 29 (2009) 2625-43.
- 377 [3] A. Erkiaga, G. Lopez, I. Barbarias, M. Artetxe, M. Amutio, J. Bilbao, et al. HDPE
378 pyrolysis-steam reforming in a tandem spouted bed-fixed bed reactor for H₂ production.
379 *Journal of Analytical and Applied Pyrolysis*. 116 (2015) 34-41.
- 380 [4] B.B. Gershman, Inc. Gasification of Non-Recycled Plastics From Municipal Solid
381 Waste In the United States. solid waste management consultants. GBB/12038 (2013).
- 382 [5] V.M.O.L. L.V. Radushkevich. Structure ugliroda, obrazujucesja pri termiceskom
383 razlozenii okisi ugliroda na zeleznom kontakte. *Zurn Fisic Chim*. 26 (1952) 88-95.
- 384 [6] S. Iijima. Helical microtubules of graphitic carbon. *Nature*. 354 (1991) 56-8.
- 385 [7] Cheaptubes. Industrial carbon nanotubes products. 2018.
- 386 [8] M. Trojanowicz. Analytical applications of carbon nanotubes: a review. *TrAC*
387 *Trends in Analytical Chemistry*. 25 (2006) 480-9.
- 388 [9] Y. Park, T. Namioka, S. Sakamoto, T.-j. Min, S.-a. Roh, K. Yoshikawa. Optimum
389 operating conditions for a two-stage gasification process fueled by polypropylene by
390 means of continuous reactor over ruthenium catalyst. *Fuel Processing Technology*. 91
391 (2010) 951-7.
- 392 [10] J. Liu, Z. Jiang, H. Yu, T. Tang. Catalytic pyrolysis of polypropylene to synthesize
393 carbon nanotubes and hydrogen through a two-stage process. *Polymer Degradation and*
394 *Stability*. 96 (2011) 1711-9.
- 395 [11] C. Wu, L. Wang, P.T. Williams, J. Shi, J. Huang. Hydrogen production from
396 biomass gasification with Ni/MCM-41 catalysts: Influence of Ni content. *Applied*
397 *Catalysis B: Environmental*. 108–109 (2011) 6-13.
- 398 [12] C. Wu, P.T. Williams. Hydrogen Production from the Pyrolysis–Gasification of
399 Polypropylene: Influence of Steam Flow Rate, Carrier Gas Flow Rate and Gasification
400 Temperature. *Energy & Fuels*. 23 (2009) 5055-61.
- 401 [13] J.C. Acomb, C. Wu, P.T. Williams. The use of different metal catalysts for the
402 simultaneous production of carbon nanotubes and hydrogen from pyrolysis of plastic
403 feedstocks. *Applied Catalysis B: Environmental*. 180 (2016) 497-510.
- 404 [14] X. Liu, Y. Zhang, M.A. Nahil, P.T. Williams, C. Wu. Development of Ni- and Fe-

405 based catalysts with different metal particle sizes for the production of carbon
406 nanotubes and hydrogen from thermo-chemical conversion of waste plastics. *Journal*
407 *of Analytical and Applied Pyrolysis*.

408 [15] T.Y. Lee, J.-H. Han, S.H. Choi, J.-B. Yoo, C.-Y. Park, T. Jung, et al. Comparison
409 of source gases and catalyst metals for growth of carbon nanotube. *Surface and*
410 *Coatings Technology*. 169–170 (2003) 348-52.

411 [16] K.A. Shah, B.A. Tali. Synthesis of carbon nanotubes by catalytic chemical vapour
412 deposition: A review on carbon sources, catalysts and substrates. *Materials Science in*
413 *Semiconductor Processing*. 41 (2016) 67-82.

414 [17] Y.C. Sui, B.Z. Cui, R. Guardián, D.R. Acosta, L. Martínez, R. Perez. Growth of
415 carbon nanotubes and nanofibres in porous anodic alumina film. *Carbon*. 40 (2002)
416 1011-6.

417 [18] S.D. Mhlanga, K.C. Mondal, R. Carter, M.J. Witcomb, N.J. Coville. The effect of
418 synthesis parameters on the catalytic synthesis of multiwalled carbon nanotubes using
419 Fe-Co/CaCO₃ catalysts. *South African Journal of Chemistry*. 62 (2009) 67-76.

420 [19] M. Kumar, Y. Ando. Controlling the diameter distribution of carbon nanotubes
421 grown from camphor on a zeolite support. *Carbon*. 43 (2005) 533-40.

422 [20] H. Ago, N. Uehara, N. Yoshihara, M. Tsuji, M. Yumura, N. Tomonaga, et al. Gas
423 analysis of the CVD process for high yield growth of carbon nanotubes over metal-
424 supported catalysts. *Carbon*. 44 (2006) 2912-8.

425 [21] G. Bajad, V. Guguloth, R.P. Vijayakumar, S. Bose. Conversion of plastic waste
426 into CNTs using Ni/Mo/MgO catalyst An optimization approach by mixture experiment.
427 *Fullerenes Nanotubes and Carbon Nanostructures*. 24 (2016) 162-9.

428 [22] N. Borsodi, A. Szentes, N. Miskolczi, C. Wu, X. Liu. Carbon nanotubes
429 synthesized from gaseous products of waste polymer pyrolysis and their application.
430 *Journal of Analytical and Applied Pyrolysis*. 120 (2016) 304-13.

431 [23] G. Che, B.B. Lakshmi, C.R. Martin, E.R. Fisher, R.S. Ruoff. Chemical Vapor
432 Deposition Based Synthesis of Carbon Nanotubes and Nanofibers Using a Template
433 Method. *Chemistry of Materials*. 10 (1998) 260-7.

434 [24] H.M. Cheng, F. Li, G. Su, H.Y. Pan, L.L. He, X. Sun, et al. Large-scale and low-
435 cost synthesis of single-walled carbon nanotubes by the catalytic pyrolysis of
436 hydrocarbons. *Applied Physics Letters*. 72 (1998) 3282-4.

437 [25] M. Golshadi, J. Maita, D. Lanza, M. Zeiger, V. Presser, M.G. Schrlau. Effects of

438 synthesis parameters on carbon nanotubes manufactured by template-based chemical
439 vapor deposition. *Carbon*. 80 (2014) 28-39.

440 [26] Z.F. Ren, Z.P. Huang, J.W. Xu, J.H. Wang, P. Bush, M.P. Siegal, et al. Synthesis of
441 large arrays of well-aligned carbon nanotubes on glass. *Science* (New York, NY). 282
442 (1998) 1105-7.

443 [27] W. Zhao, B. Basnet, I.J. Kim. Carbon nanotube formation using zeolite template
444 and applications. *Journal of Advanced Ceramics*. 1 (2012) 179-93.

445 [28] X. Liu, H. Sun, C. Wu, D. Patel, J. Huang. Thermal Chemical Conversion of High-
446 Density Polyethylene for the Production of Valuable Carbon Nanotubes Using Ni/AAO
447 Membrane Catalyst 2017.

448 [29] M. Lee, B. Wang, Z. Wu, K. Li. Formation of micro-channels in ceramic
449 membranes – Spatial structure, simulation, and potential use in water treatment. *Journal*
450 *of Membrane Science*. 483 (2015) 1-14.

451 [30] E.T. Thostenson, Z. Ren, T.-W. Chou. Advances in the science and technology of
452 carbon nanotubes and their composites: a review. *Composites Science and Technology*.
453 61 (2001) 1899-912.

454 [31] N. Labhsetwar, P. Doggali, S. Rayalu, R. Yadav, T. Mistuhashi, H. Haneda.
455 *Ceramics in Environmental Catalysis: Applications and Possibilities*. *Chinese Journal*
456 *of Catalysis*. 33 (2012) 1611-21.

457 [32] C. Quan, N. Gao, C. Wu. Utilization of NiO/porous ceramic monolithic catalyst
458 for upgrading biomass fuel gas. *Journal of the Energy Institute*.

459 [33] N. Gao, S. Liu, Y. Han, C. Xing, A. Li. Steam reforming of biomass tar for
460 hydrogen production over NiO/ceramic foam catalyst. *International Journal of*
461 *Hydrogen Energy*. 40 (2015) 7983-90.

462 [34] Y. Liu, M. Peng, H. Jiang, W. Xing, Y. Wang, R. Chen. Fabrication of ceramic
463 membrane supported palladium catalyst and its catalytic performance in liquid-phase
464 hydrogenation reaction. *Chemical Engineering Journal*. 313 (2017) 1556-66.

465 [35] J.W. An, D.H. You, D.S. Lim. Tribological properties of hot-pressed alumina–CNT
466 composites. *Wear*. 255 (2003) 677-81.

467 [36] E. Flahaut, A. Peigney, C. Laurent, C. Marlière, F. Chastel, A. Rousset. Carbon
468 nanotube–metal–oxide nanocomposites: microstructure, electrical conductivity and
469 mechanical properties. *Acta Materialia*. 48 (2000) 3803-12.

470 [37] V. Muñoz, A.G.T. Martinez. Thermal Evolution of Al₂O₃-MgO-C Refractories.

471 Procedia Materials Science. 1 (2012) 410-7.

472 [38] J. Zygmuntowicz, P. Wiecińska, A. Miazga, K. Konopka. Characterization of
473 composites containing NiAl₂O₄ spinel phase from Al₂O₃/NiO and Al₂O₃/Ni systems.
474 Journal of Thermal Analysis and Calorimetry. 125 (2016) 1079-86.

475 [39] C. Wu, M.A. Nahil, M. Norbert, J. Huang, P.T. Williams. Production and
476 application of carbon nanotubes, as a co-product of hydrogen from the pyrolysis-
477 catalytic reforming of waste plastic. Process Safety and Environmental Protection.

478 [40] W.Z. Li, J.G. Wen, Z.F. Ren. Effect of temperature on growth and structure of
479 carbon nanotubes by chemical vapor deposition. Applied Physics A. 74 (2002) 397-
480 402.

481 [41] G.L. Hornyak, A.C. Dillon, P.A. Parilla, J.J. Schneider, N. Czap, K.M. Jones, et al.
482 Template synthesis of carbon nanotubes. Nanostructured Materials. 12 (1999) 83-8.

483 [42] A. Aqel, K.M.M.A. El-Nour, R.A.A. Ammar, A. Al-Warthan. Carbon nanotubes,
484 science and technology part (I) structure, synthesis and characterisation. Arabian
485 Journal of Chemistry. 5 (2012) 1-23.

486 [43] F. Danafar, A. Fakhru'l-Razi, M.A.M. Salleh, D.R.A. Biak. Fluidized bed catalytic
487 chemical vapor deposition synthesis of carbon nanotubes—A review. Chemical
488 Engineering Journal. 155 (2009) 37-48.

489 [44] B.R. Stoner, B. Brown, J.T. Glass. Selected Topics on the Synthesis, Properties
490 and Applications of Multiwalled Carbon Nanotubes. Diamond and related materials.
491 42 (2014) 49-57.

492 [45] K.-E. Kim, K.-J. Kim, W.S. Jung, S.Y. Bae, J. Park, J. Choi, et al. Investigation on
493 the temperature-dependent growth rate of carbon nanotubes using chemical vapor
494 deposition of ferrocene and acetylene. Chemical Physics Letters. 401 (2005) 459-64.

495 [46] C.J. Lee, J. Park, Y. Huh, J. Yong Lee. Temperature effect on the growth of carbon
496 nanotubes using thermal chemical vapor deposition. Chemical Physics Letters. 343
497 (2001) 33-8.

498 [47] N. Mishra, G. Das, A. Ansaldo, A. Genovese, M. Malerba, M. Povia, et al.
499 Pyrolysis of waste polypropylene for the synthesis of carbon nanotubes. Journal of
500 Analytical and Applied Pyrolysis. 94 (2012) 91-8.

501 [48] C. Wu, P.T. Williams. Pyrolysis–gasification of post-consumer municipal solid
502 plastic waste for hydrogen production. International Journal of Hydrogen Energy. 35
503 (2010) 949-57.

504 [49] J.C. Acomb, C. Wu, P.T. Williams. Effect of growth temperature and
505 feedstock:catalyst ratio on the production of carbon nanotubes and hydrogen from the
506 pyrolysis of waste plastics. *Journal of Analytical and Applied Pyrolysis*. 113 (2015)
507 231-8.

508 [50] A.F.I.-R. Hengameh Hanaei^{1, 2,*}, Dayang Radiah Awang Biak², Intan Salwani
509 Ahamad² and Firoozeh Danafar. Effects of Synthesis Reaction Temperature,
510 Deposition Time and Catalyst on Yield of Carbon Nanotubes. *Asian Journal of*
511 *Chemistry*. 24 (2010) 2407-14.

512 [51] T. Setareh Monshi, A. Fakhru'l-Razi, A. Luqman Chuah, A.R. Suraya.
513 Optimization of Synthesis Condition for Carbon Nanotubes by Catalytic Chemical
514 Vapor Deposition (CCVD). *IOP Conference Series: Materials Science and Engineering*.
515 17 (2011) 012003.

516 [52] E.F. Kukovitsky, S.G. L'Vov, N.A. Sainov, V.A. Shustov, L.A. Chernozatonskii.
517 Correlation between metal catalyst particle size and carbon nanotube growth. *Chemical*
518 *Physics Letters*. 355 (2002) 497-503.

519 [53] S.B. Sinnott, R. Andrews, D. Qian, A.M. Rao, Z. Mao, E.C. Dickey, et al. Model
520 of carbon nanotube growth through chemical vapor deposition. *Chemical Physics*
521 *Letters*. 315 (1999) 25-30.

522 [54] Y. Li, W. Kim, Y. Zhang, M. Rolandi, D. Wang, H. Dai. Growth of Single-Walled
523 Carbon Nanotubes from Discrete Catalytic Nanoparticles of Various Sizes. *The Journal*
524 *of Physical Chemistry B*. 105 (2001) 11424-31.

525 [55] C.L. Cheung, A. Kurtz, H. Park, C.M. Lieber. Diameter-Controlled Synthesis of
526 Carbon Nanotubes. *The Journal of Physical Chemistry B*. 106 (2002) 2429-33.

527 [56] A.L.M. da Silva, J.P. den Breejen, L.V. Mattos, J.H. Bitter, K.P. de Jong, F.B.
528 Noronha. Cobalt particle size effects on catalytic performance for ethanol steam
529 reforming – Smaller is better. *Journal of Catalysis*. 318 (2014) 67-74.

530 [57] F. Danafar, A. Fakhru'l-Razi, M.A. Mohd Salleh, D.R. Awang Biak. Influence of
531 catalytic particle size on the performance of fluidized-bed chemical vapor deposition
532 synthesis of carbon nanotubes. *Chemical Engineering Research and Design*. 89 (2011)
533 214-23.

534 [58] A. Gorbunov, O. Jost, W. Pompe, A. Graff. Role of the catalyst particle size in the
535 synthesis of single-wall carbon nanotubes. *Applied Surface Science*. 197–198 (2002)
536 563-7.

- 537 [59] C. Lastoskie, K.E. Gubbins, N. Quirke. Pore size distribution analysis of
538 microporous carbons: a density functional theory approach. *The Journal of Physical*
539 *Chemistry*. 97 (1993) 4786-96.
- 540 [60] R.J.W. R.T.K. Baker. Formation of carbonaceous deposits from the platinum-iron
541 catalyzed decomposition of acetylene. *Journal of Catalysis*. 37 (1975) 101-5.
- 542 [61] D. Baudouin, U. Rodemerck, F. Krumeich, A.d. Mallmann, K.C. Szeto, H. Ménard,
543 et al. Particle size effect in the low temperature reforming of methane by carbon dioxide
544 on silica-supported Ni nanoparticles. *Journal of Catalysis*. 297 (2013) 27-34.
- 545 [62] D. Chen, K.O. Christensen, E. Ochoa-Fernández, Z. Yu, B. Tøtdal, N. Latorre, et
546 al. Synthesis of carbon nanofibers: effects of Ni crystal size during methane
547 decomposition. *Journal of Catalysis*. 229 (2005) 82-96.
- 548 [63] D. Venegoni, P. Serp, R. Feurer, Y. Kihn, C. Vahlas, P. Kalck. Parametric study for
549 the growth of carbon nanotubes by catalytic chemical vapor deposition in a fluidized
550 bed reactor. *Carbon*. 40 (2002) 1799-807.
- 551 [64] F. Melo, N. Morlanés. Naphtha steam reforming for hydrogen production.
552 *Catalysis Today*. 107–108 (2005) 458-66.

553

554

555

556

557

558

Table 1 - ICP results of Ni/ceramic catalysts with different Ni contents				
catalysts	0.1 / ceramic	0.5 / ceramic	1.0 / ceramic	2.0 / ceramic
Ni content wt.%	0.25	1.1	2.1	3.3

559

560

561

562

563

564

565

566

567

568

569

570

571

572

573

574

575

576

577

578

579

580

581

582

Table 2 – Overall view of experiments parameters and carbon depositions

	Ni Content ($molL^{-1}$)	Temperature ($^{\circ}C$)	Amorphous Carbon (%)	Filamentous Carbon (%)	CNTs Average Diameter (nm)
Effect of the Ni content	0.1	700	1.1	3.1	15.7 \pm 3.6
	0.5	700	1.2	6.0	16.9 \pm 4.3
	1.0	700	2.0	9.4	20.8 \pm 1.9
	2.0	700	2.2	8.0	24.9 \pm 2.3
Effect of temperature	0.5	600	2.1	7.2	21.2 \pm 5.6
	0.5	700	1.2	6.0	16.9 \pm 4.3
	0.5	800	1.2	1.2	-

583

584

585

586

587

588

589

590

591

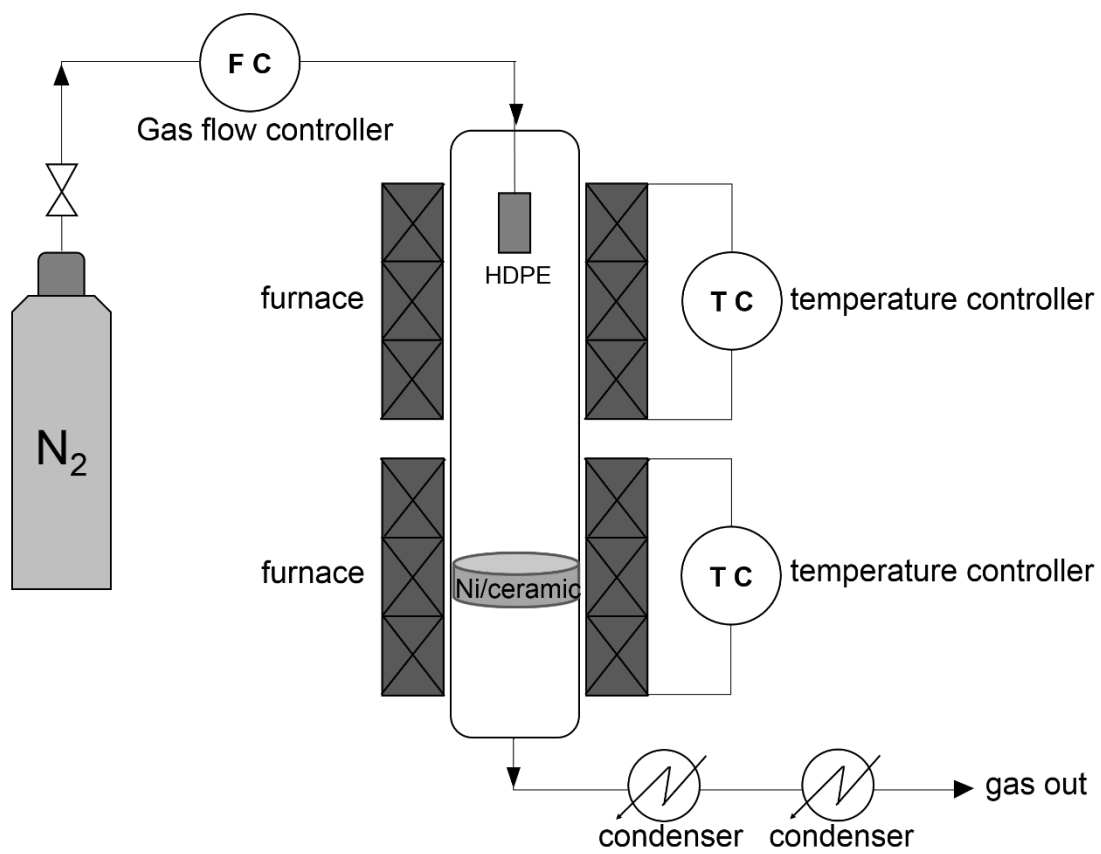
592

593

594

595

596



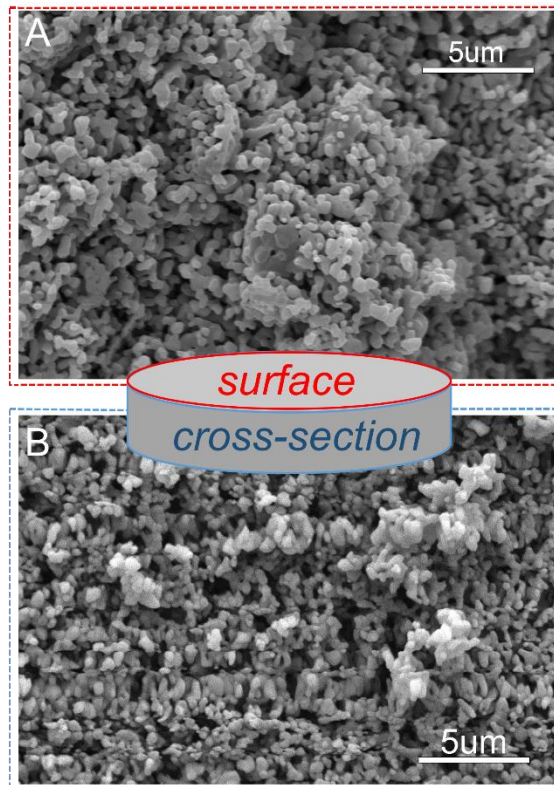
597

598 Fig. 1 A schematic diagram of the reactor for the synthesis CNTs from waste plastics

599

600

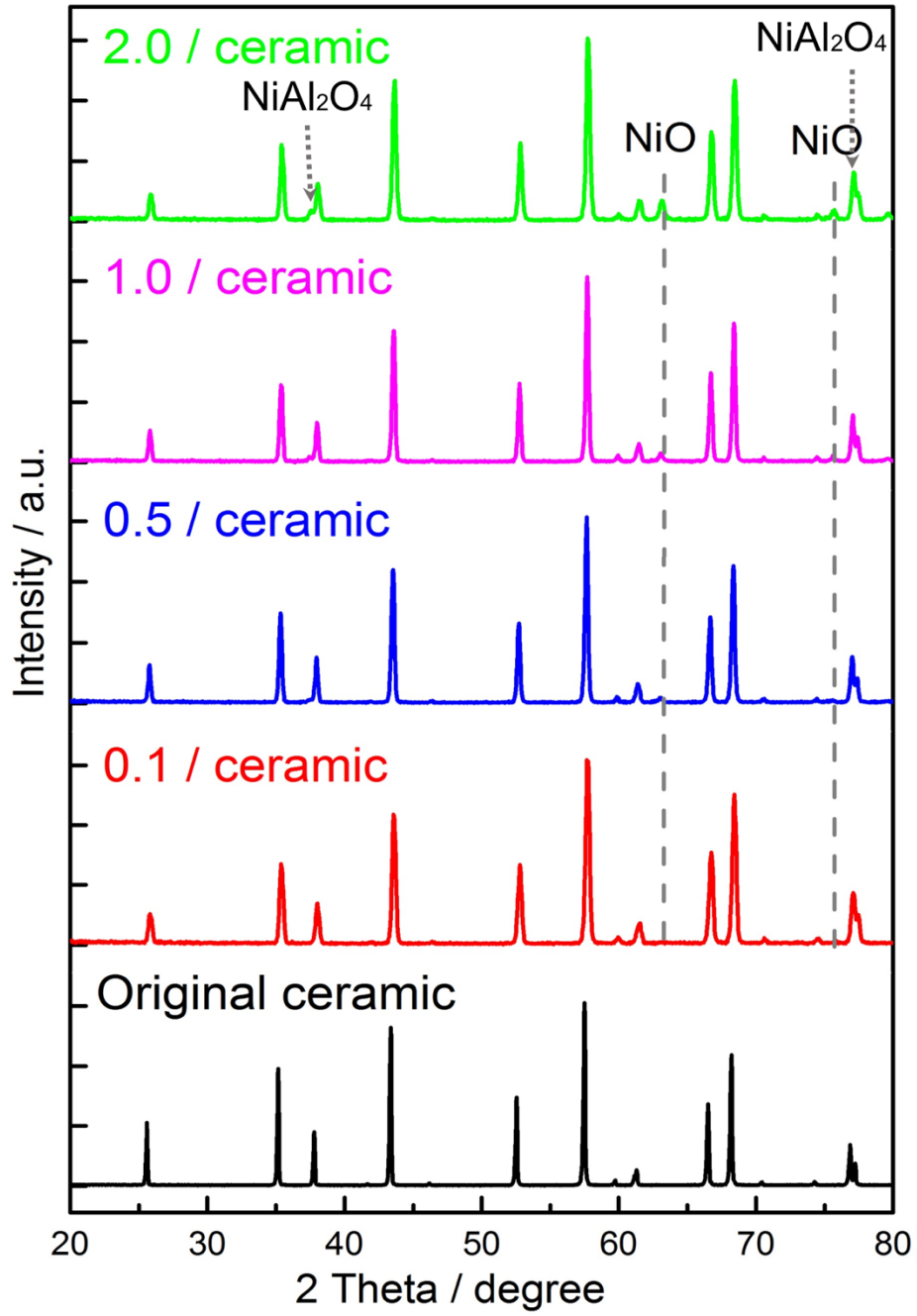
601



602

603 Fig. 2 SEM results for original ceramic membrane (A) surface, (B) cross-section

604



605

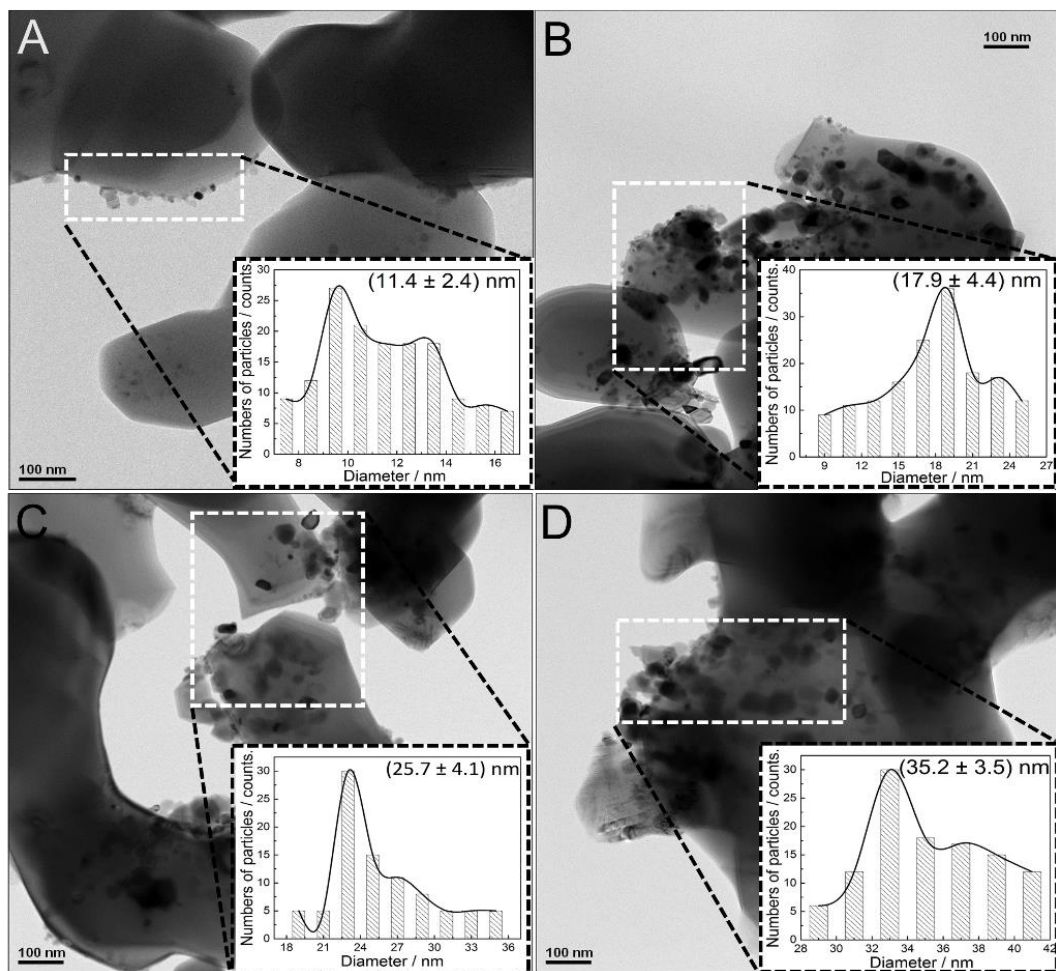
606 Fig. 3 XRD analysis for original ceramic membrane and fresh Ni/ceramic catalysts

607

608

609

610



612

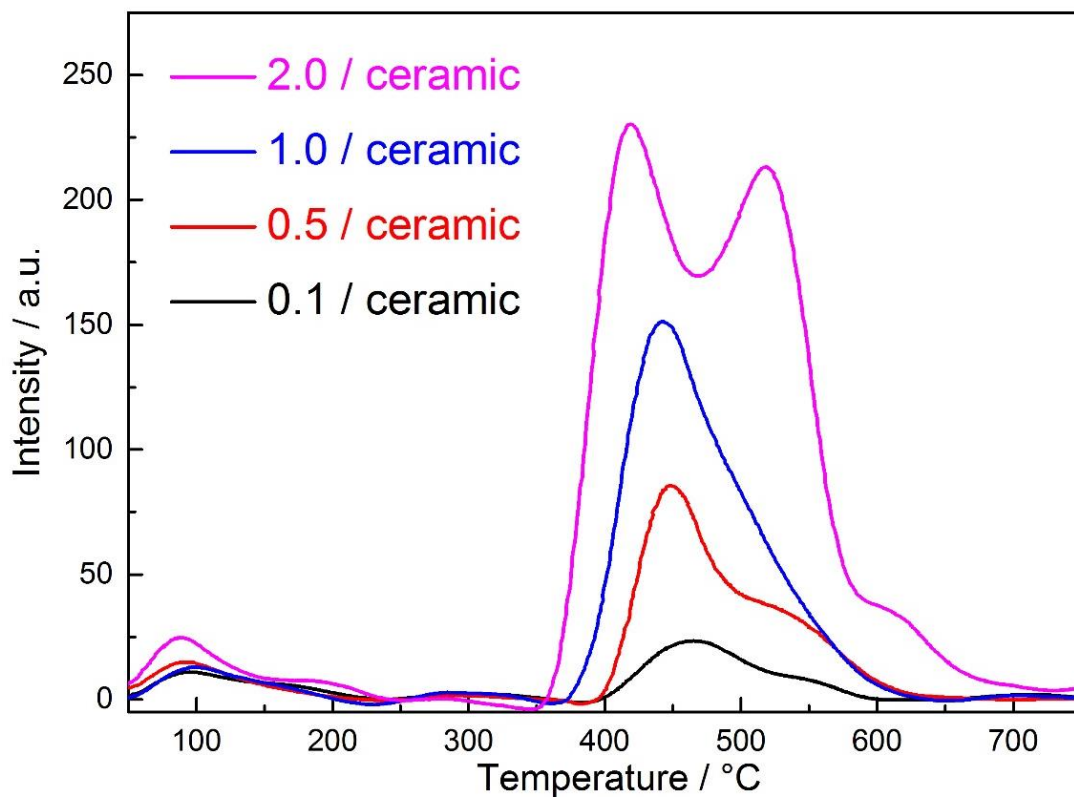
613 Fig. 4 TEM results and diameter distribution of NiO for (A) 0.1, (B) 0.5, (C) 1.0 and

614

(D) 2.0 fresh Ni/ceramic catalysts

615

616



617

618 Fig. 5 TPR analysis of the Ni/ceramic catalysts with different Ni content loadings

619

(0.1, 0.5, 1.0, and 2.0 Ni mol/L)

620

621

622

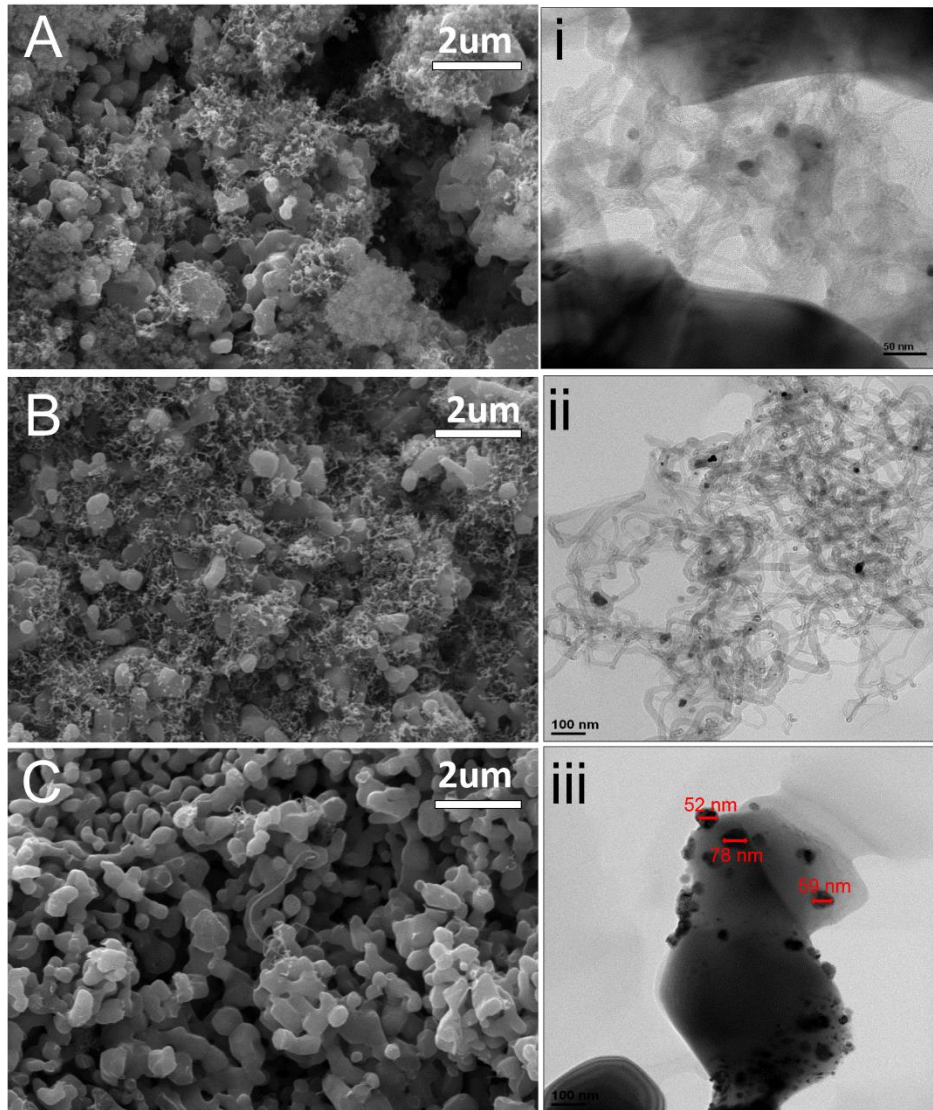
623

624

625

626

627



628

629 Fig. 6 SEM (left) and TEM (right) results for CNTs synthesis at (A) 600°C, (B) 700°C

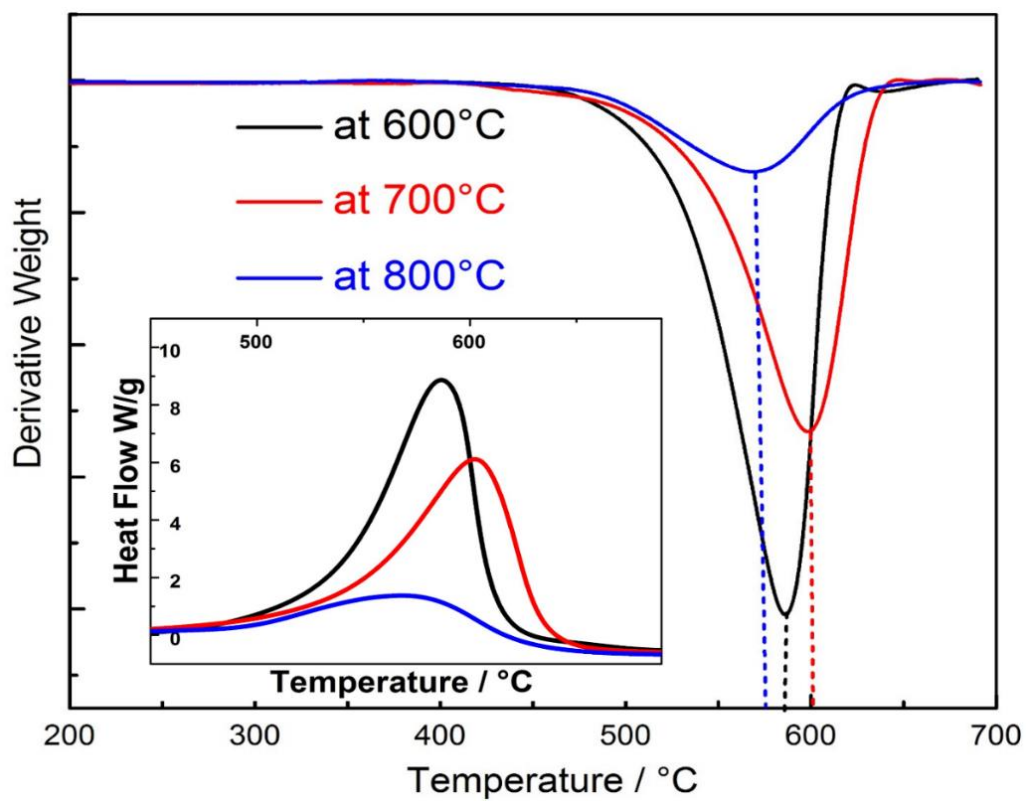
630

and (C) 800°C

631

632

633



634

635 Fig. 7 DTG-TPO and DSC results of the spent 0.5/ceramic at 600 °C, 700 °C, and

636

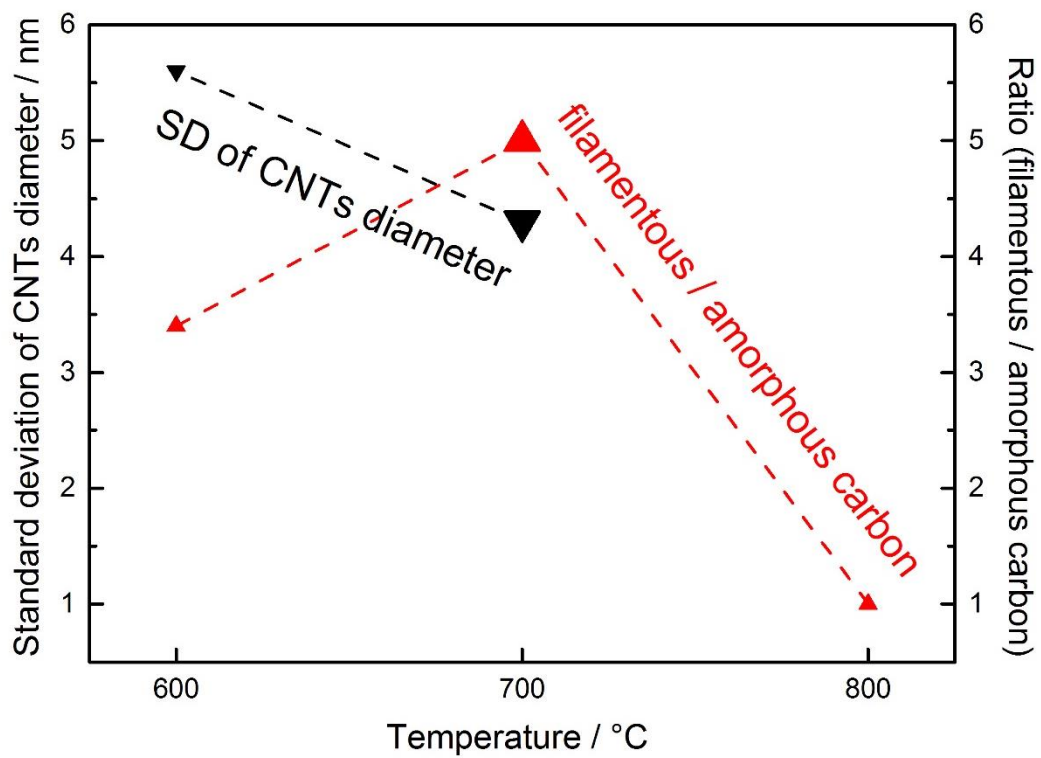
800 °C

637

638

639

640



641

642

Fig. 8 Trends of standard deviation (SD) of CNTs diameter and

643

filamentous/amorphous carbon ratio at 600 °C, 700 °C, and 800 °C

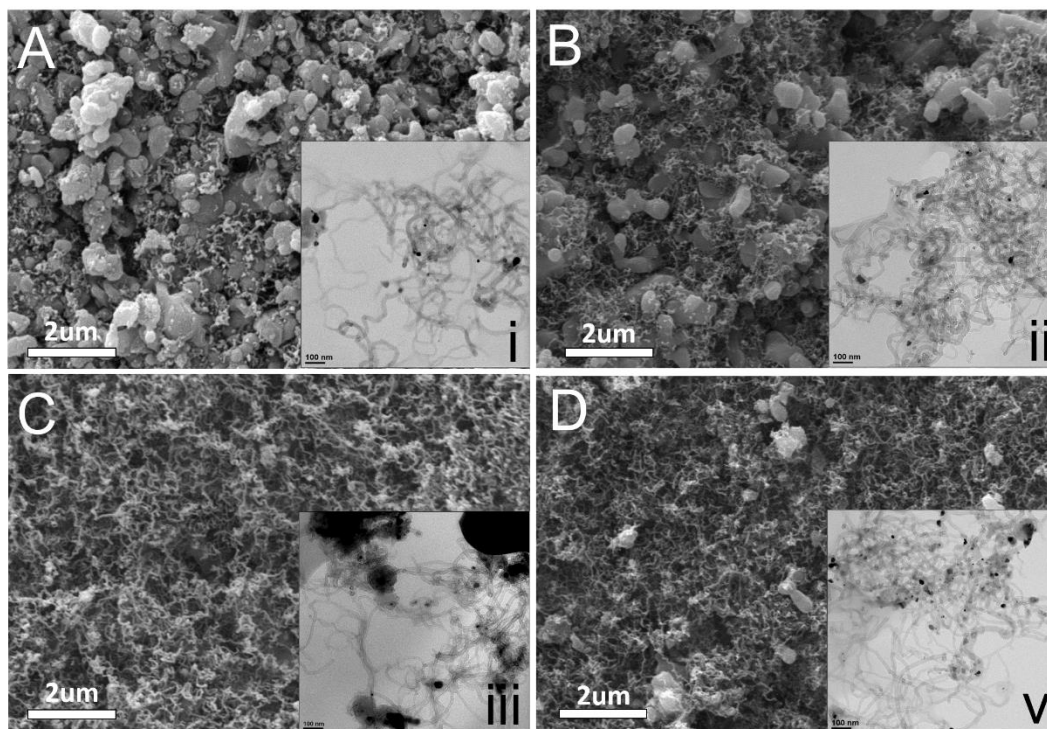
644

645

646

647

648



649

650

Fig. 9 SEM results of CNTs formation for 0.1/ceramic (A), 0.5/ceramic (B),

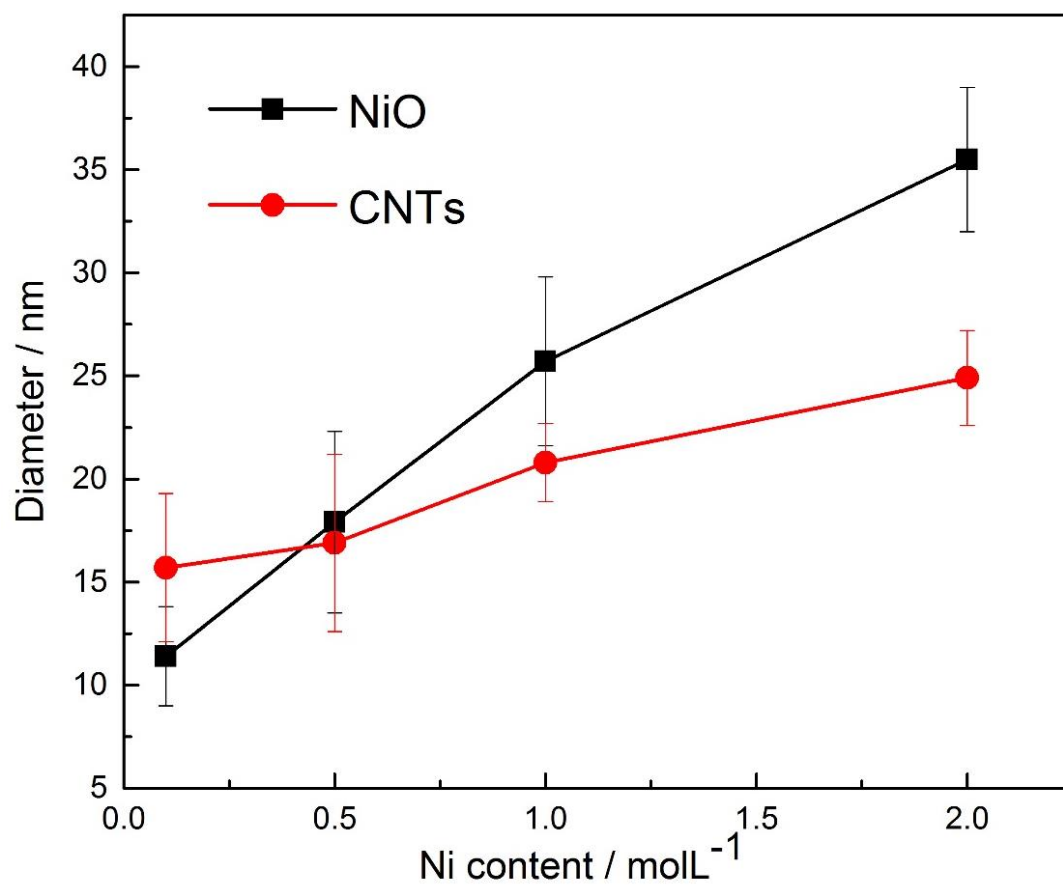
651

1.0/ceramic (C), and 2.0/ceramic (D) and corresponding TEM (i-v)

652

653

654



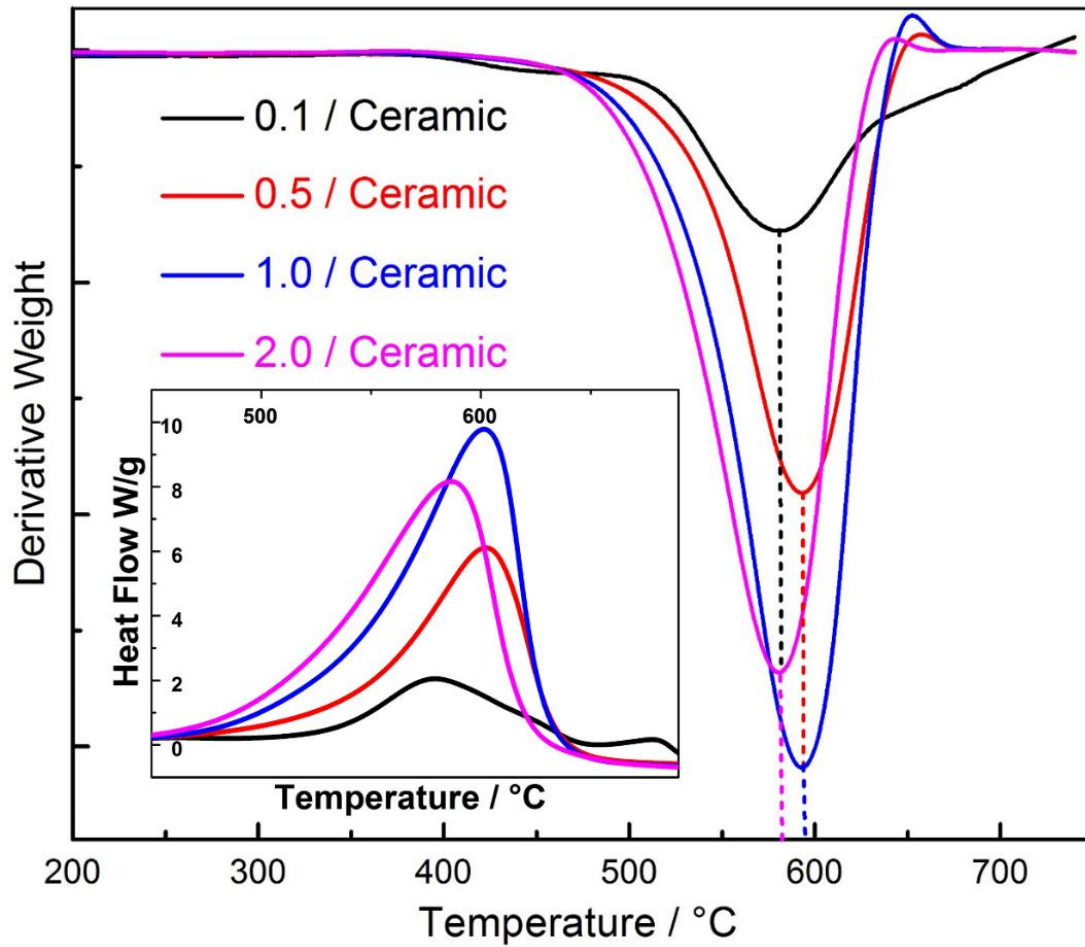
655

656 Fig. 10 Diameter distribution comparison for fresh and spent Ni/ceramic catalysts

657

658

659



660

661 Fig. 11 DTG-TPO and DSC results of the spent 0.1/ceramic, 0.5/ceramic, 1.0/ceramic

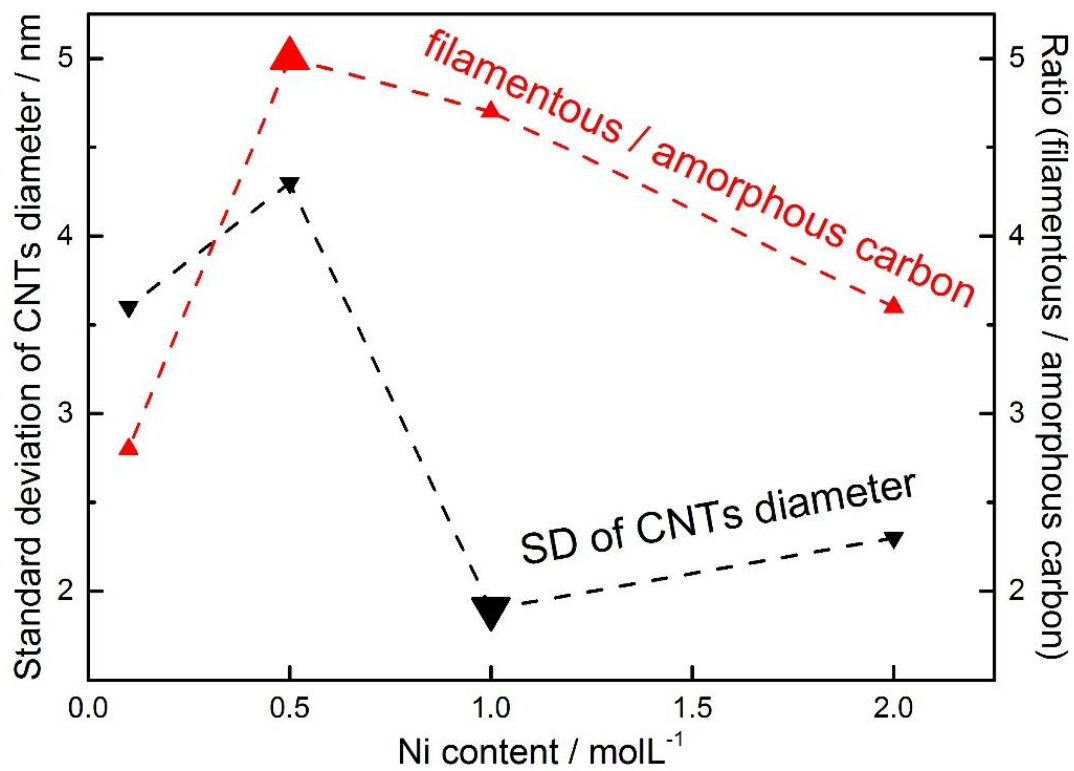
662 and 2.0/ceramic catalysts at 700 °C

663

664

665

666



667

668

669

670

Fig. 12 Trends of standard deviation (SD) of CNTs diameter and filamentous/amorphous carbon ratio with different Ni loading ceramic catalysts